PHYSICAL REVIEW D **74,** 094502 (2006)

Nonperturbative U(1) gauge theory at finite temperature

Bernd A. Berg and Alexei Bazavov

Department of Physics, Florida State University, Tallahassee, Florida 32306-4350, USA
School of Computational Science, Florida State University, Tallahassee, Florida 32306-4120, USA
(Received 30 May 2006; published 1 November 2006)

For compact U(1) lattice gauge theory we have performed a finite size scaling analysis on $N_\tau N_s^3$ lattices for N_τ fixed by extrapolating spatial volumes of size $N_s \leq 18$ to $N_s \to \infty$. Within the numerical accuracy of the thus-obtained fits, we find for $N_\tau = 4$, 5 and 6 second order critical exponents, which exhibit no obvious N_τ dependence. The exponents are consistent with 3d Gaussian values, but not with either first order transitions or the universality class of the 3d XY model. As the 3d Gaussian fixed point is known to be unstable, the scenario of a yet unidentified nontrivial fixed point close to the 3d Gaussian emerges as one of the possible explanations.

DOI: 10.1103/PhysRevD.74.094502 PACS numbers: 11.15.Ha, 11.10.Wx, 12.38.Aw

I. INTRODUCTION

Abelian, compact U(1) gauge theory has played a prominent role in our understanding of the permanent confinement of quarks. It was first investigated by Wilson in his 1974 milestone paper [1], which introduced lattice gauge theory (LGT). For a 4d hypercubic lattice, his U(1) action reads

$$S(\{U\}) = \sum_{\square} S_{\square} \tag{1}$$

with $S_{\square} = \mathrm{Re}(U_{i_1 j_1} U_{j_1 i_2} U_{i_2 j_2} U_{j_2 i_1})$, where i_1, j_1, i_2, and j_2 label the sites circulating about the square $\square$ and the U_{ij} are complex numbers on the unit circle, $U_{ij} = \exp(i\phi_{ij})$, $0 \leq \phi_{ij} < 2\pi$.

Wilson concluded that at strong couplings the theory confines static test charges due to an area law for the path ordered exponentials of the gauge field around closed paths (Wilson loops). A hypothetical mechanism of confinement was identified by Polyakov [2], who attributed it in 3d Abelian gauge theory to the presence of a monopole plasma. For the 4d theory at weak coupling, both Wilson and Polyakov expected a Coulomb phase in which the test charges are not confined. The existence of two distinct phases was later rigorously proven [3].

So it comes as no surprise that 4d U(1) LGT was the subject of one of the very early Monte Carlo (MC) calculations in LGT [4]. One simulates a 4d statistical mechanics with the Boltzmann factor $\exp[-\beta_g S(\{U\})]$ and periodic boundary conditions (other boundary conditions are possible too, but are not considered here); $\beta_g = 1/g^2$ is related to the gauge coupling g^2, $\beta_g = 0$ is the strong coupling limit, and $\beta_g \to \infty$ is the weak coupling limit. The study [4] allowed one to identify the confined and deconfined phases. After some debate about the order of the phase transition, the bulk transition on symmetric lattices was suggested to be (weakly) first order [5], a result which was substantiated by simulations of the Wuppertal group [6,7]. Other investigations followed up on the topological properties of the theory. This lies outside the scope of the present paper. The interested reader may trace this literature from [8].

The particle excitations of 4d U(1) LGT are called gauge balls and, in the confined phase, also glueballs. Their masses were first studied in Ref. [9]. In the confined phase all masses decrease when one approaches the transition point. Crossing it, they rise in the Coulomb phase with the exception of the axial vector mass, which is consistent with the presence of a massless photon in that phase. Recently, this picture was confirmed in Ref. [10], relying on far more powerful computers and efficient noise reduction techniques [11]. The first order nature of the transition prevents one from reaching a continuum limit, as is seen in Fig. 7 of [10]. In contrast to that, investigations in a spherical geometry [12] and of an extended U(1) Wilson action [13] reported a scaling behavior of glueballs consistent with a second order phase transition. But this is challenged in other papers [14,15], so that it remains questionable whether an underlying nontrivial quantum field theory of the confined phase can be defined in this way.

Here we focus on U(1) LGT in finite temperature geometries. We consider the Wilson action (1), choose units $a = 1$ for the lattice spacing, and perform MC simulations on $N_\tau N_s^3$ lattices. Testing U(1) code for our biased Metropolis-heatbath updating (BMHA) [16], we noted on small lattices that the characteristics of the first order phase transition disappeared when we went from the $N_\tau = N_s$ to a $N_\tau N_s^3$, $N_\tau < N_s$ geometry. This motivated us to embark on a finite size scaling (FSS) calculation of the critical exponents of U(1) LGT in the $N_\tau N_s^3$, $N_\tau =$ constant, $N_s \to \infty$ geometry. For a review of FSS methods and scaling relations, see [17].

Later we learned about a paper by Vettorazzo and de Forcrand [18], who speculate about a scenario of two transitions at finite, fixed N_τ: One for confinement-deconfinement, another one into the Coulomb phase, both coinciding only for the zero temperature transition. Their claim for the confinement-deconfinement transition

is that it is first order for $N_\tau = 8$ and 6, $N_s \to \infty$, becoming so weak for $N_\tau \leq 4$ that it might then be second order. In contrast to having two transitions at finite N_τ, the conventional expectation appears to be one transition, which is first order for sufficiently large N_τ. For small N_τ it may be second order and is then conjectured to be in the 3d XY universality class. See Svetitsky and Yaffe [19] for an early discussion of some of these points.

In the next section we present our numerical results in comparison with previous literature, followed by a summary and conclusions in the final section.

II. NUMERICAL RESULTS

Our FSS analysis relies on multicanonical simulations [20] for which the parameters were determined using a modification of the Wang-Landau (WL) recursion [21]. A speed-up by a factor of about 3 was achieved by implementing the biased Metropolis-heatbath algorithm [16] for the updating instead of relying on the usual Metropolis procedure. This is substantial as, for instance, our 16^4 lattice run takes about 80 days on a 2 GHz PC. Additional overrelaxation [22] sweeps were used for some of the simulations.

TABLE I. Statistics of our MC calculations. The simulation with $*$ attached in the WL column uses 22 WL recursions, all others 20.

						Cycles	
L_τ	L	WL	Sweeps/run	$\beta_{\min}$	$\beta_{\max}$	1	2
4	4	18 597	$32 \times 20\,000$	0.0	1.2	213	240
4	4	11 592	$32 \times 20\,000$	0.8	1.2	527	594
4	5	14 234	$32 \times 12\,000$	0.8	1.2	146	172
4	6	19 546	$32 \times 32\,000$	0.9	1.1	258	364
4	8	29 935	$32 \times 32\,000$	0.95	1.05	229	217
4	10	25 499	$32 \times 64\,000$	0.97	1.03	175	317
4	12	47 379	$32 \times 112\,000$	0.98	1.03	338	360
4	14	44 879	$32 \times 112\,000$	0.99	1.02	329	322
4	16	54 623	$32 \times 128\,000$	0.99	1.02	19	219
4	18	58 107	$32 \times 150\,000$	0.994	1.014	93	259
5	5	18 201	$32 \times 12\,000$	0.8	1.2	114	122
5	6	20 111	$32 \times 36\,000$	0.9	1.1	294	308
5	8	31 380	$32 \times 40\,000$	0.95	1.05	35	191
5	10	47 745	$32 \times 72\,000$	0.97	1.03	144	231
5	12	37 035	$32 \times 112\,000$	0.99	1.02	280	326
5	14	49 039	$32 \times 112\,000$	1.0	1.02	192	277
5	16	43 671	$32 \times 160\,000$	1.0	1.02	226	257
5	18	56 982	$32 \times 180\,000$	1.0	1.014	138	241
6	6	28 490	$32 \times 40\,000$	0.9	1.1	312	281
6	8	44 024	$32 \times 40\,000$	0.96	1.04	173	175
6	10	51 391	$32 \times 72\,000$	0.97	1.04	139	170
6	12	41 179	$32 \times 128\,000$	0.995	1.02	226	283
6	14	50 670	$32 \times 128\,000$	1.0	1.02	89	220
6	16	56 287	$32 \times 160\,000$	1.0	1.02	149	189
6	18	68 610	$32 \times 180\,000$	1.005	1.015	123	200
8	8	46 094	$32 \times 40\,000$	0.97	1.03	111	159
10	10	48 419	$32 \times 96\,000$	0.98	1.03	103	133
12	12	70 340	$32 \times 112\,000$	0.99	1.03	75	82
14	14	112 897	$32 \times 128\,000$	1.0	1.02	57	51
16	16	87 219	$32 \times 160\,000$	1.007	1.015	12	73
16	16	191 635*	$32 \times 160\,000$	1.007	1.015	48	74

Our temporal lattice extensions are $N_\tau = 4$, 5 and 6. For N_s our values are 4, 5, 6, 8, 10, 12, 14, 16 and 18. Besides, we have simulated symmetric lattices up to size 16^4. The statistics analyzed in this paper is shown in Table I. The lattice sizes are collected in the first and second columns. The third column contains the number of sweeps spent on the WL recursion for the multicanonical parameters. Typically the parameters are frozen after reaching $f = e^{1/20}$ for the multiplicative WL factor (technical details of our procedure will be published elsewhere). Column four lists our production statistics from simulations with fixed multicanonical weights. Columns five and six give the β values between which our Markov process cycled. Adapting the definition of chapter 5.1 of [23], one cycle takes the process from the configuration space region at $\beta_{\min}$ to $\beta_{\max}$ and back. Each run was repeated once more, where after the first run the multicanonical parameters were estimated from the statistics of this run. Columns seven and eight give the number of cycling events recorded during runs 1 and 2.

Using the logarithmic coding of chapter 5.1.5 of [23], physical observables are reweighted to canonical ensembles. Error bars as shown in the figures are calculated using jackknife bins (e.g., chapter 2.7 of [23]) with their number given by the first value in column four (always 32), while the second value was also used for the number of equilibrium sweeps (without measurements) performed after the recursion. Weighted by the number of their completed cycles, the results from two or more runs are combined for the final analysis (compare chapter 2.1.2 of [23]).

A. Action variables

Figures 1 and 2 show for various values of N_s the specific heat

$$C(\beta) = \frac{1}{6N}[\langle S^2\rangle - \langle S\rangle^2] \quad \text{with} \quad N = N_\tau N_s^3 \qquad (2)$$

in the neighborhood of the phase transition for $N_\tau = 6$ and on symmetric lattices. The β ranges in the figures are chosen to match.

In Fig. 3 we show all our specific heat maxima on a log-log scale. Our data for the symmetric lattices are for $N_s \geq 8$ consistently described by a fit to the first order transition form [24] $C_{\max}(N_s)/(6N) = c_0 + a_1/N + a_2/N^2$. The goodness of our fit is $Q = 0.64$ (see, e.g., chapter 2.8 of Ref. [23] for the definition and a discussion of Q), and its estimate for the specific heat density is $c_0 = 0.000\,196\,1\,(26)$. This is 10% higher than the c_0 value reported by the Wuppertal group [7], where lattices up to size 18^3 were used. For the interface tension, consistent fits

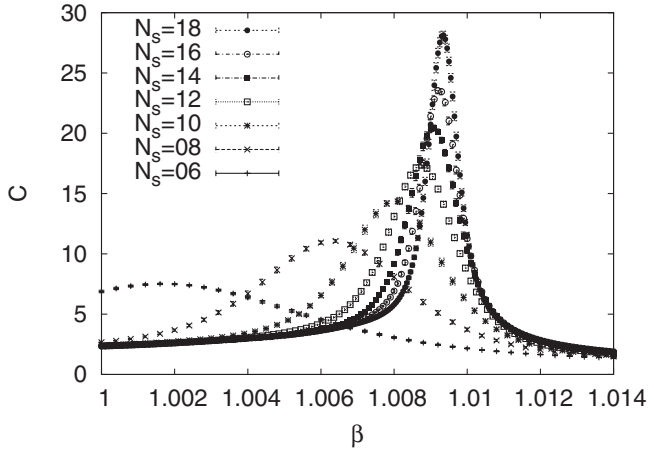

FIG. 1. Finite size dependence of the specific heat functions $C(\beta)$ on $N_\tau = 6$ lattices.

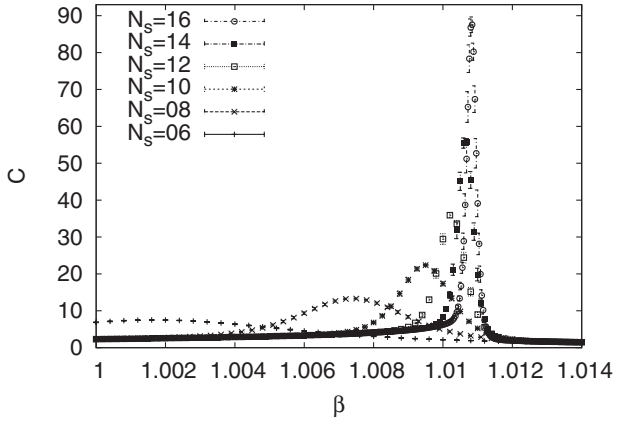

FIG. 2. Finite size dependence of the specific heat functions $C(\beta)$ on $N_\tau = N_s$ lattices.

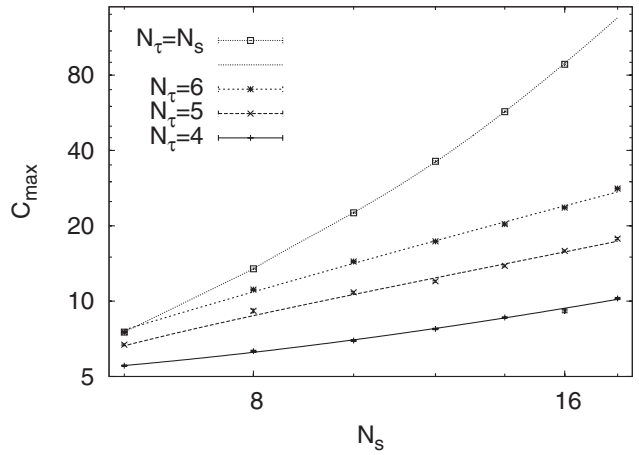

FIG. 3. Maxima of the specific heat.

to a small positive as well as to a zero infinite volume value are possible. Interestingly, the Wuppertal group decided against including their largest lattices from [6] in their final analysis [7], because action data on them did not cover the double peak region coherently (communicated by T. Neuhaus).

For $N_\tau = 4$, 5 and 6, our curves in Fig. 3 are linear fits in N_s, $C_{\max}(N_s) = a_1 N_s + a_0 + a_{-1}/N_s$. For $N_\tau = 4$, the goodness of this fit is $Q = 0.20$ using our $N_s \geq 6$ data. But for $N_\tau = 5$ and 6, the Q values are unacceptably small, although the data scatter nicely about the curves. For large N_s, the maxima of the specific heat curves scale like (see [17])

$$C_{\max}(N_s) \sim N_s^{\alpha/\nu}, \tag{3}$$

where one has $\alpha/\nu = 4$ in the case of the first order transition for $N_\tau = N_s$. In the N_τ fixed, $N_s \to \infty$ geometry, the systems become three dimensional, so that $\alpha/\nu = 3$ would be indicative of a first order transition, while our data are consistent with the second order exponent $\alpha/\nu = 1$.

This has to be contrasted with the claim by Vettorazzo and de Forcrand [18] that the $N_\tau \geq 6$ transitions are first order. For $N_\tau = 8$ and 6, their evidence relies on simulations of very large lattices. Differences in action values obtained after ordered and disordered starts support a nonzero latent heat in the infinite volume limit. For $N_\tau = 6$, the spatial lattice sizes used are $N_s = 48$ and 60 and their MC statistics shown consists of 5000 measurements per run, separated by one heatbath plus four overrelaxation sweeps (these units are not defined in [18], but were communicated to us by de Forcrand and previously used in [15]). For a second order phase transition, the integrated autocorrelation time τ_{int} scales approximately $\sim N_s^2$ and we estimate from our own simulations on smaller lattices that in units of those measurements $\tau_{\text{int}} \approx 7000$ for $N_\tau = 6$ and $N_s = 48$. A MC segment of the length of τ_{int} delivers one statistically independent event (e.g., chapter 4.1.1 of [23]). Therefore, the run of [18] would, in the case of a second order transition, be based on less than one event, and strong metastabilities would be expected as soon as the Markov chain approaches the scaling region. For $N_s = 60$ and the $N_\tau = 8$ lattices, the situation is even worse. We conclude that these data cannot decide the order of the transition.

Let us remind the reader that a double peak alone does not signal a first order transition. One has to study its FSS behavior, but no error bars can be estimated when one has only one statistically independent event. Actually, for our larger spatial volumes we find double peaks in our $6 \times N_s^3$ action histograms and they are also well known to occur for the magnetization of the 3d Ising model at its critical point [25].

B. Polyakov loop variables

Besides the action, we measured Polyakov loops and their low-momentum structure factors. For U(1) LGT, Polyakov loops are the U_{ij} products along the straight lines in the N_τ direction. Each Polyakov loop $P_{\vec{x}}$ is a complex number on the unit circle, which depends only on the space coordinates, quite like an XY spin in 3d. We calculate the sum over all Polyakov loops on the lattice

$$P = \sum_{\vec{x}} P_{\vec{x}}. \tag{4}$$

The critical exponent γ/ν is obtained from the maxima of the susceptibility of the absolute value $|P|$,

$$\chi_{\max} = \frac{1}{N_s^3}[\langle |P|^2\rangle - \langle |P|\rangle^2]_{\max} \sim N_s^{\gamma/\nu}, \tag{5}$$

and $(1-\beta)/\nu$ from the maxima of

$$\chi^{\beta}_{\max} = \frac{1}{N_s^3}\frac{d}{d\beta}\langle |P|\rangle \Big|_{\max} \sim N_s^{(1-\beta)/\nu}. \tag{6}$$

Structure factors are defined by (see, e.g., Ref. [26])

$$F(\vec{k}) = \frac{1}{N_s^3}\left\langle \left| \sum_{\vec{r}} P(\vec{r}) \exp(i\vec{k}\,\vec{r}) \right|^2 \right\rangle, \qquad \vec{k} = \frac{2\pi}{N_s}\vec{n}, \tag{7}$$

where $\vec{n}$ is an integer vector, which is, for our measurements, restricted to (0,0,1), (0,1,0), and (1,0,0). Maxima of structure factors scale like

$$F_{\max}(\vec{k}) \sim N_s^{2-\eta}. \tag{8}$$

The exponents can be estimated from two parameter fits, (A) $Y = a_1 N_s^{a_2}$. Because of finite size corrections, the goodness Q of these fits will be too small when all lattice sizes are included. The strategy is then not to overweight [27] the small lattices and to omit, starting with the smallest, lattices altogether until an acceptable $Q \geq 0.05$ has been reached. We found a rather slow convergence of the thus-obtained estimates with increasing lattice size. This can be improved by including more parameters in the fit. So we used the described strategy also for three parameter fits, (B) $Y = a_0 + a_1 N_s^{a_2}$. The penalty for including more parameters is, in general, increased instability against fluctuations of the data and, in particular, their error bars. For a number of our data sets, this is the case for fit B, so that an extension to more than three parameters makes no sense. We performed first the fit B for each data set, but did fall back to fit A when no consistency or stability was reached for a fit B including at least the five largest lattices. The thus-obtained values are listed in Table II. Table III gives additional information about the fits.

Our lattices support second order transitions for $N_\tau = 4$, 5 and 6. The evidence is best for observables derived from Polyakov loops. For example, in Fig. 4 we show our data for the maxima of the Polyakov loop susceptibility together with their fits used in Table II (for the symmetric lattices the data are connected by straight lines). For fixed N_τ we find an approximately quadratic increase with N_s, while there is a decrease for the symmetric lattices, which appears to converge towards zero or a finite discontinuity (note that one has no common scale for Polyakov loops from symmetric lattices, because their lengths change with N_τ).

TABLE II. Estimates of critical exponents as explained in the text. Properties of the fits are summarized in Table III.

N_τ	α/ν	γ/ν	$(1-\beta)/\nu$	$2-\eta$
4	1.15 (10)	1.918 (34)	1.39 (7)	1.945 (10)
5	0.97 (04)	2.086 (79)	1.51 (4)	1.955 (20)
6	1.31 (07)	1.968 (37)	1.59 (4)	1.901 (31)
nt	1.15 (15)	1.95 (5)	1.55 (5)	1.95 (5)

TABLE III. Number of data used and type of fit (A or B as explained in text), goodness of fit Q.

N_τ	α/ν	γ/ν	$(1-\beta)/\nu$	$2-\eta$
4	7B, 0.25	7B, 0.21	7B, 0.25	8B, 0.78
5	4A, 0.76	6B, 0.40	4A, 0.80	7B, 0.23
6	3A, 0.09	7B, 0.09	4A, 0.83	5B, 0.42

Our structure factor data support the Coulomb phase for $\beta > \beta_c$: As shown for $N_\tau = 6$ in Fig. 5 the structure factors remain divergent for $\beta > \beta_c$, as expected for a power law fall-off of Polyakov loop correlations. These observations apply to the β ranges (compare Table I) covered by our multicanonical simulations. To have still many cycling events on large lattices, this range was chosen to shrink with increasing lattice size. So we do not test very far into the $\beta > \beta_c$ phase.

The Polyakov loops describe 3d spin systems. One would like to identify whether the observed transitions are in any of their known universality classes. At first

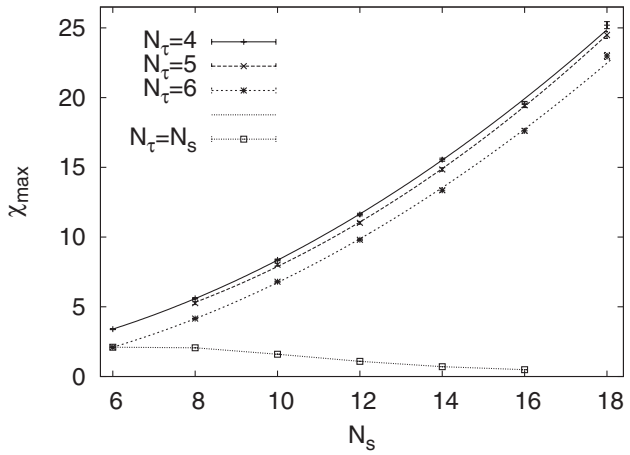

FIG. 4. Maxima of Polyakov loop susceptibilities.

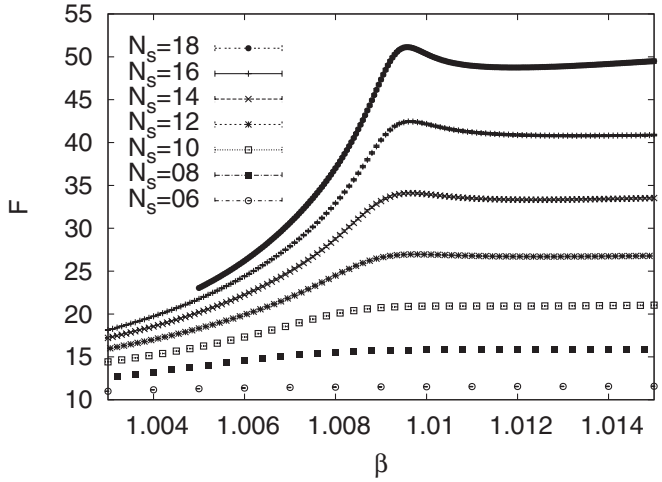

FIG. 5. Structure factors (7) for $N_\tau = 6$.

thought, the universality class of the 3d XY model comes to mind (e.g., [19]), because the symmetry is correct. It is easy to see that the $N_\tau = 1$ gauge system decouples into a 3d XY model and a 3d U(1) gauge theory. The latter has no transition and is always confined. But one cannot learn much from this observation, as there is no interaction between the two systems. Surprisingly, the data of Table II do not support the XY universality class. Although our estimates of γ/ν agree with what is expected, α/ν is entirely off. For the XY model, a small negative value is established [17], while Fig. 3 shows that all our specific heat maxima increase steadily. We remark that the scenario may change for $N_\tau < 4$. We have preliminary results for $N_\tau = 2$ and 3. The increase of the specific heat maxima becomes considerably weaker than for $N_\tau = 4$. For $N_\tau = 2$ it slows continuously down with increasing lattice size (so far up to $N_s = 20$) and one can imagine that it comes altogether to a halt. Once completed, our simulations for $N_\tau = 2$ and 3 will be reported elsewhere.

III. SUMMARY AND CONCLUSIONS

In view of expected systematic errors due to our limited lattice sizes, one can state that our estimates of Table II are consistent with the Gaussian values $\alpha/\nu = 1$ and $\gamma/\nu = 2$ (with error bars 0.3 for α/ν and 0.1 for γ/ν). Using the hyperscaling relation $2 - \alpha = d\nu$ with $d = 3$ yields $\alpha = \nu = 1/2$. The other estimates of exponents listed in Table II provide consistency checks, as they are linked to $\alpha/\nu = 1$ and $\gamma/\nu = 2$ by the scaling relations $\alpha + 2\beta + \gamma = 2$ and $\gamma/\nu = 2 - \eta$. For the Gaussian exponents, $(1 - \beta)/\nu = 1.5$ and $\eta = 0$ follow, both consistent with the data of the table.

However, the problem with the Gaussian scenario is that the Gaussian renormalization group fixed point in 3d has two relevant operators [28], so one does not understand why the effective spin system should care to converge into this fixed point [19]. Therefore, the interesting scenario of a new nontrivial (nt) fixed point with exponents accidentally close to the 3d Gaussian arises. An illustration, which is consistent with the data, is given in the last row of Table II. The mean values are constructed to fulfill the scaling relations and match with $\nu = 0.482$, $\alpha = 0.554$, $\gamma = 0.94$, $\beta = 0.253$, $\eta = 0.05$.

One may expect that the first order transition of the symmetric lattices prevails once N_τ is larger than the correlation length on symmetric lattices. But a nonzero interface tension has never been established for this transition. So one could also imagine an instability under the change of the geometry. From a FSS point of view, it appears then natural that the character of the transition will not change anymore, once a value of N_τ has been reached, which is sufficiently large to be insensitive to lattice artifacts. Up to normalizations data from $N_\tau N_s^3$ and $2N_\tau(2N_s)^3$, $N_s > N_\tau$ lattices should then become quite similar. We illustrate this here by rescaling the maxima of our Polyakov loop susceptibilities with a common factor, so that they become equal to 1 on symmetric lattices. On a log-log scale the results are then plotted in Fig. 6 against N_s/N_τ. The behavior is consistent with assuming a common critical exponent for all of them (parallel lines are then expected for large N_s/N_τ).

The litmus test for identifying a second order phase transition is that one is able to calculate its critical exponents unambiguously. Instead of starting with data of uncontrolled quality from very large lattices, the FSS strategy is to control finite size effects by working from small systems up to large systems. With MC calculations, FSS methods find their limitations through the lattice sizes, which fit into the computer and can be accurately simulated in a reasonable time. Within the multicanonical approach, ''accurately'' means that one has to get the system cycling through the entire critical or first order region, and at least about 100 cycles ought to be completed with measurements.

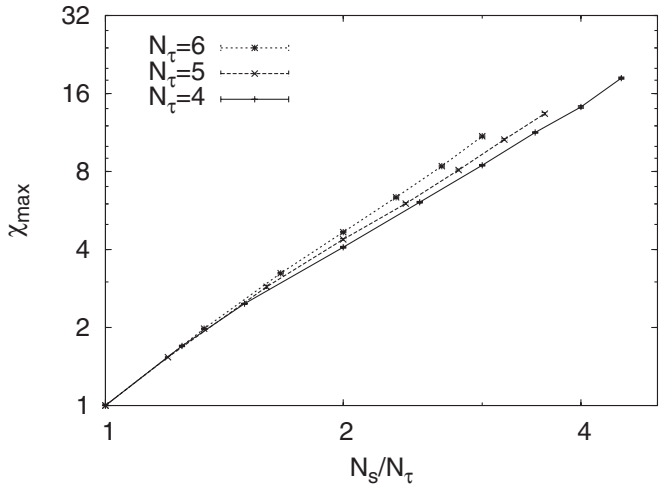

FIG. 6. Rescaled maxima of Polyakov loop susceptibilities.

Our lattice sizes are not small on the scale of typical numerical work on U(1) LGT, for instance, the lattices used for the Wuppertal c_0 estimate of [7]. But we have not yet reached lattices large enough to provide hard evidence that there is no $N_s \to \infty$ turnaround towards either a first order transition or the 3d XY fixed point. In particular, in view of the fact that our data do not support the generally expected scenario, it would be desirable to extend the present analysis to the largest lattices that can be reached by extensive simulations on supercomputers, instead of relying on relatively small PC clusters.

With mass spectrum methods [10,29] one may investigate the scaling behavior of the model from a different angle. In particular, observation of a massless photon [9] can provide more direct evidence for the Coulomb phase than our structure factor measurements. Finally, renormalization group theory could contribute to clarifying the issues raised by our data. Amazingly, even after more than 30 years since Wilson's paper [1], the nature of the U(1) LGT phase transition is still not entirely understood.

ACKNOWLEDGMENTS

We thank Urs Heller for checking on one of our action distributions with his own code and Thomas Neuhaus for communicating details of the Wuppertal data. We are indebted to Philippe de Forcrand for email exchanges and useful discussions. This work was in part supported by the US Department of Energy under Contract No. DE-FA02-97ER41022. Our data were generated on PC clusters at FSU.

[1] K. G. Wilson, Phys. Rev. D **10**, 2445 (1974).
[2] A. M. Polyakov, Phys. Lett. **59B**, 82 (1975).
[3] A. H. Guth, Phys. Rev. D **21**, 2291 (1980).
[4] M. Creutz, L. Jacobs, and C. Rebbi, Phys. Rev. D **20**, 1915 (1979).
[5] J. Jersak, T. Neuhaus, and P. M. Zerwas, Phys. Lett. **133B**, 103 (1983).
[6] G. Arnold, T. Lippert, T. Neuhaus, and K. Schilling, Nucl. Phys. B, Proc. Suppl. **94**, 651 (2001).
[7] G. Arnold, B. Bunk, T. Lippert, and K. Schilling, Nucl. Phys. B, Proc. Suppl. **119**, 864 (2003), and references given therein.
[8] Y. Koma, M. Koma, and P. Majumdar, Nucl. Phys. **B692**, 209 (2004); M. Panero, J. High Energy Phys. 05 (2005) 66.
[9] B. A. Berg and C. Panagiotakopoulos, Phys. Rev. Lett. **52**, 94 (1984).
[10] P. Majumdar, Y. Koma, and M. Koma, Nucl. Phys. **B677**, 273 (2004).
[11] L. Lüscher and P. Weisz, J. High Energy Phys. 09 (2001) 10.
[12] J. Jersak, C. B. Lang, and T. Neuhaus, Phys. Rev. D **54**, 6909 (1996).
[13] J. Cox, W. Franzki, J. Jersak, H. Pfeiffer, C. B. Lang, T. Neuhaus, and P. W. Stephenson, Nucl. Phys. **B499**, 371 (1997); J. Cox, J. Jersak, H. Pfeiffer, T. Neuhaus, P. W. Stephenson, and A. Seyfried, Nucl. Phys. **B545**, 607 (1999), and references given therein.
[14] I. Campos, A. Cruz, and A. Tarancón, Nucl. Phys. **B528**, 325 (1998).
[15] M. Vettorazzo and P. de Forcrand, Nucl. Phys. **B686**, 85 (2004).
[16] A. Bazavov and B. A. Berg, Phys. Rev. D **71**, 114506 (2005).
[17] A. Pelissetto and E. Vicari, Phys. Rep. **368**, 549 (2002).
[18] M. Vettorazzo and P. de Forcrand, Phys. Lett. B **604**, 82 (2004).
[19] B. Svetitsky and L. G. Yaffe, Nucl. Phys. **B210**, 423 (1982).
[20] B. A. Berg and T. Neuhaus, Phys. Rev. Lett. **68**, 9 (1992).
[21] F. Wang and D. P. Landau, Phys. Rev. Lett. **86**, 2050 (2001).
[22] S. L. Adler, Phys. Rev. D **37**, 458 (1988).
[23] B. A. Berg, *Markov Chain Monte Carlo Simulations and Their Statistical Analysis* (World Scientific, Singapore, 2004).
[24] C. Borgs and R. Kotecky, Phys. Rev. Lett. **68**, 1734 (1992), and references given therein.
[25] K. Binder, Z. Phys. B **43**, 119 (1981).
[26] H. E. Stanley, *Introduction to Phase Transitions and Critical Phenomena* (Clarendon Press, Oxford, 1971), p. 98.
[27] As MC runs on small lattices are "cheap," one tends to have more accurate data for them than for the valuable large lattices. Care should be taken that the error-to-signal ratios are similar for all included lattice sizes.
[28] For example, F. J. Wegner, in *Phase Transitions and Critical Phenomena*, edited by C. Domb and M. S. Green (Academic Press, New York, 1976), p. 59.
[29] L. Tagliacozzo, hep-lat/0603022 [Phys. Lett. B (to be published)].